Article ID: 1006-8775(2020) 02-0125-12

The Relationship Between Abnormal Meiyu and Medium−Term Scale Wave Perturbation Energy Propagation Along the East Asian Subtropical Westerly Jet

JIN Rong-hua (金荣花) [1], YANG Ning (杨 宁) [2], SUN Xiao-qing (孙晓晴) [2], LIU Si-jia (刘思佳) [3], YIN Shan (尹 姗) [1]

(1. National Meteorological Center, China Meteorological Administration, Beijing 100081 China;
2. School of Atmospheric Sciences, Chengdu University of Information Technology, Chengdu 610225 China;
3. Chengdu Plateau Meteorological Institute, China Meteorological Administration, Chengdu 610072 China)

Abstract: The East Asian subtropical westerly jet (EASWJ) is one of the most important factors modulating the Meiyu rainfall in the Yangtze-Huaihe River Basin, China. This article analyzed periods of the medium-term EASWJ variation, wave packet distribution and energy propagation of Rossby waves along the EASWJ during Meiyu season, and investigated their possible influence on abnormal Meiyu rain. The results showed that during the medium-term scale atmospheric dynamic process, the evolution of the EASWJ in Meiyu season was mainly characterized by the changes of 3−8 d synoptic-scale and 10−15 d low-frequency Rossby waves. The strong perturbation wave packet and energy propagation of the 3−8 d synoptic-scale and 10−15 d low-frequency Rossby waves are mostly concentrated in the East Asian region of 90°−150°E, where the two wave trains of perturbation wave packets and wave-activity flux divergence coexist in zonal and meridional directions, and converge on the EASWJ. Besides, the wave trains of perturbation wave packet and wave-activity flux divergence in wet Meiyu years are more systematically westward than those in dry Meiyu years, and they are shown in the inverse phases between each other. In wet (dry) Meiyu year, the perturbation wave packet high-value area of the 10−15 d low-frequency variability is located between the Aral Sea and the Lake Balkhash (in the northeastern part of China), while over eastern China the wave-activity flux is convergent and strong (divergent and weak), and the high-level jets are strong and southward (weak and northward). Because of the coupling of high and low level atmosphere and high-level strong (weak) divergence on the south side of the jet over the Yangtze-Huaihe River Basin, the low-level southwest wind and vertically ascending motion are strengthened (weakened), which is (is not) conducive to precipitation increase in the Yangtze-Huaihe River Basin. These findings would help to better understand the impact mechanisms of the EASWJ activities on abnormal Meiyu from the perspective of medium-term scale Rossby wave energy propagation.

Key words: East Asian subtropical westerly jet (EASWJ); medium-term scale; Rossby wave; wave packet distribution; energy propagation; abnormal Meiyu

CLC number: P442 **Document code:** A

https://doi.org/10.46267/j.1006-8775.2020.012

1 INTRODUCTION

The subtropical high-level westerly jet is a strong and narrow high-speed airflow belt in the upper troposphere over subtropical regions, being quasi-horizontal in three-dimensional space with strong vertical and lateral boundary wind shear (Berggren et al. [1]; Endlich and Mclean [2]). The maximum wind speed center of the subtropical high-level jet appears near the break zone in the mid-latitude tropopause, where the Hadley circulation in the upper troposphere and the Ferrel circulation over the mid-latitude join each other (Huang and Yu [3]), linking momentum and heat exchange between middle and low latitudes and playing a very important role in the conservation of global atmospheric angular momentum and energy (Gao et al. [4-5]; Patrick [6]). The subtropical high-level jet has three maximum wind speed centers in the Northern Hemisphere, located respectively over East Asia, North America and the Middle East, among which the center over East Asia is the strongest (Ding et al. [7]; Tan et al. [8]) and the transient eddy change in its exit zone is the largest (Lau and Boyle [9]). This is known as the East Asian subtropical westerly jet (EASWJ). Researchers have revealed that the EASWJ, as an important component of the East Asian monsoon circulation (Tao and Wei [10]), has a significant influence on the seasonal transition of East Asian atmospheric circulation (Ye et al. [11]; Sheng [12]), the onset of Asian summer monsoon (Chen [13]; Chen et al. [14]), and the summer rainfall in eastern China (Tao et al. [15-6]; Li et al. [17]; Kuang and Zhang [18]; Jin et al. [19];

Received 2019-10-14; **Revised** 2020-02-15; **Received** 2020-05-15

Funding: National Natural Science Foundation of China (41575066); National Science and Technology Support Program of China (2015BAC03B04)

Biography: JIN Rong-hua, Ph. D., primarily undertaking research on weather analysis and large-scale dynamics.

Corresponding author: JIN Rong-hua, e-mail: jinrh@cma.gov.cn.

Guo and Zhang [20]; Zhang et al. [21]).

The tropopause in tropical and subtropical regions is an important area for the propagation of Rossby waves and the subtropical jet acts as a waveguide (Hoskins and Karoly [22]; Hoskins and Ambrizzi [23]). The Asian jet waveguide extends from North Africa to the western coast of North America and its intensity diminishes spirally (Ambrizzi et al. [24]). Chang [25] pointed out that the subtropical jet in the upper troposphere was the strongest baroclinic waveguide over the Asian continent in the Northern Hemisphere in summer, and the baroclinic waves propagating along the Asian jet were more coherent than those in other regions. In the jet waveguide, synoptic-scale wave packets propagate from west to east, causing a downstream dispersion effect. Terao [26] showed that the Rossby waves propagating along the jet waveguide dominated the mode of seasonal variation in the mid-latitudes of the Northern Hemisphere in summer. Lu et al. [27] found that the teleconnection pattern along the Asian subtropical westerly jet (ASWJ) in July was a possible linkage of the East Asian summer monsoon and the Indian monsoon. Nitta [28], Huang and Li [29], and Huang and Sun [30-31] found that the dispersion of quasi-stationary Rossby waves formed East Asia-Pacific (EAP) or Pacific-Japan (PJ) teleconnection wave trains, which impacted greatly on weather and climate in Asia and even the whole globe. Therefore, the distribution of Asian summer rainfall can be investigated by studying the energy dispersion of Rossby waves. Tao et al. [32] pointed out that the downstream development effect of Rossby wave trains contributed significantly to the severe flooding in China. The energy propagation process of Rossby waves along the ASWJ is an important driving force for the development of East Asian high-level troughs and the Western Pacific subtropical high. Mei and Guan [33] demonstrated that the baroclinic waves form wave packets that propagate downstream, and had an obvious downstream dispersion effect. The high-frequency baroclinic waves originated from near the Caspian Sea, spreading downstream along the ASWJ. The perturbation energy brought by the baroclinic wave packets provided enough energy for the generation and development of heavy rains in the Yangtze River Basin. Xu et al. [34] found that Rossby wave energy could be dispersed eastward via the teleconnection wave trains over the Eurasian continent, strengthening the East Asian monsoon system and affecting the climate change in East Asia. In 2003, the World Meteorological Organization (WMO) put forward the THORPEX (The Observing System Research and Predictability Experiment) program, aiming at improving the accuracy of high-impact weather forecasts with lead time of 1 day to 2 weeks. This program pointed out that successfully predicting the cyclone development in the vicinity of Japan and the subsequent Rossby wave energy dispersion is crucial for improving the capability of the medium-range forecasting of the European flood event. However, as mentioned above, previous studies mainly analyzed the Rossby wave activity along the subtropical jet and its influence on Meiyu based on a case of a certain weather process, lacking systematic studies, let alone the exploration of scientific problems from the medium scale.

In this study, focusing on the 2-week medium-term scale during the Meiyu season, we will analyze the impact of the anomalous EASWJ activities on Meiyu rain in the Yangtze-Huaihe River Basin of China on the basis of the perturbation wave packet and energy propagation of Rossby waves. The rest of the paper is organized as follows. Section 2 describes the data and methodologies. Section 3 presents the period of the medium-term EASWJ variation during the Meiyu season. Section 4 and 5 display the distribution of perturbation wave packets and energy propagation of Rossby waves along the EASWJ, respectively. Section 6 discusses their impacts on abnormal circulation in the Meiyu season. The results are summarized in Section 7.

2 MATERIALS AND METHODS

The NCEP / NCAR (National Center for Environmental Prediction /National Center for Atmospheric Research) 2.5° × 2.5° daily reanalysis data, collected from 1960 to 2015, with 17 layers in 1,000−10 hPa vertically are used (Kalnay et al. [35]). This spatial resolution is sufficient to the analysis of the medium-term weather processes featured by large scales. The daily precipitation data are from 2,426 national weather stations of the China National Station network, China Meteorological Administration (CMA). According to the Meiyu rain monitoring data of the National Climate Center (CMA) (Xu et al. [36]) and our previous research (Jin et al. [37]), a year is defined as wet Meiyu year when the standard deviation of Meiyu rainfall is bigger than 1.0, or as dry Meiyu year when the rainfall and circulation conditions fail to meet the Meiyu criteria. Therefore, from 1960 to 2015, seven years are wet Meiyu years and four are dry Meiyu years. The years of 1969, 1980, 1983, 1991, 1996, 1998 and 1999 are wet Meiyu years and the years of 1965, 2000, 2002 and 2009 are dry Meiyu years. The data period for this study is from June to July of the Meiyu season across the Yangtze-Huaihe River Basins during these years (Ding et al. [38]; Li et al. [39]).

The Morlet wavelet method (Torrence and Compo [40]) is used to analyze the significant period of the EASWJ time series and to extract the medium-term scale of the EASWJ perturbation. This medium-term scale is also the time domain of narrow-band signal of the following bandpass filtering.

The size of the wave packet value can reflect the strength of the perturbation energy of the wave (Ge et al. [41]; Xiao et al. [42]). The wave packet value of the narrow-band signal is obtained by using Hilbert

transform of the narrow-band signal (Miao et al. [43]). The specific calculation steps for the sec value are as follows.

(1) The narrow-band signal $P(x,y,t)$ of the 200 hPa zonal wind field is obtained by using the bandpass filtering method.

$$P(x, y, t) = A(x, y, t) \cdot \cos[kx+ly+\omega_0 t+\varphi(x, y, t)] \quad (1)$$

(2) Finding the Hilbert transform $\hat{P}(x, y, t)$ of a known narrow-band signal $P(x, y, t)$ is actually to find the orthogonal sequence of the known narrow-band signal sequence, namely:

$$\hat{P}(x, y, t) = A(x, y, t) \cdot \sin[kx+ly+\omega_0 t+\varphi(x, y, t)] \quad (2)$$

(3) Finding the amplitude of analytic signal $P_c(x, y, t)$ is to find the envelope of the narrow-band signal, and the wave packet value of the narrow-band signal, i.e.,

$$\left|P_c(x,y,t)\right| = A(x,y,t)\,, \quad (3)$$

where,

$$\mathbf{W} = \frac{P}{2|U|}\begin{vmatrix} U(\psi_x'^2 - \psi'\psi_{xx}') + V(\psi_x'\psi_y' - \psi'\psi_{xy}') \\ U(\psi_x'\psi_y' - \psi'\psi_{xy}') + V(\psi_y'^2 - \psi'\psi_{yy}') \\ \frac{f_0^2}{S^2}\left| U(\psi_x'\psi_p' - \psi'\psi_{xp}') + V(\psi_y'\psi_p' - \psi'\psi_{yp}')\right| \end{vmatrix}, \quad (4)$$

where $\mathbf{W}$ is wave-activity flux, ψ' is quasi-geotropic perturbation flow function, U and V are basic flow fields, P is pressure divided by 1000 hPa, $|U|$ is climatic value of horizontal wind speed, and S^2 is static stability parameter. The divergence of $\mathbf{W}$ is expressed by

$$\nabla \cdot \mathbf{W} = \frac{\partial \mathbf{W}_x}{\partial_x} + \frac{\partial \mathbf{W}_y}{\partial_y}. \quad (5)$$

Under westerly conditions, the direction of this wave-activity flux $\mathbf{W}$ is the same as that of the energy propagation, and also as that of the group velocity (the moving velocity of the wave packet), and the magnitude of the absolute value of the vector $\mathbf{W}$ is proportional to the energy propagation speed. When $\nabla \cdot \mathbf{W}>0$, the wave-activity flux is divergent, indicating the output of wave activity and the average westerly wind is strengthened.

$$P_c(x,y,t) = P(x,y,t) + i\hat{P}(x,y,t),$$

$$A(x,y,t) = \sqrt{P^2(x,y,t) + \hat{P}^2(x,y,t)}.$$

(4) The wave packet values of the obtained spatial points are drawn into a wave packet distribution map, and then the wave packet characteristics are obtained through analyzing the wave packet distribution map. In this paper, the zonal wind field of 200 hPa has been standardized, and the wave packet values obtained are dimensionless.

Based on the work of Plumb [44], Takaya and Nakamura [45] reported a wave-activity flux, i. e., $\mathbf{W}$, containing uneven basic zonal flow. The wave-activity flux $\mathbf{W}$ is an effective parameter for studying wave energy propagation, wave-flow interaction and geostrophic potential vorticity transport, and is also an important diagnostic tool for planetary wave activities and anomalies (Eliassen and Palm [46]; Huang [47]; Li [48-49]).

In contrast, when $\nabla \cdot \mathbf{W}<0$, the wave-activity flux is convergent, representing the convergence of wave activity and weakening of the average westerly wind.

3 PERIODS OF THE MEDIUM−TERM EASWJ VARIATION

Analyzing the 200 hPa zonal wind and its standard deviation distribution during June-July, 1960−2015 (Fig. 1), we find that the 120° E jet axis of the EASWJ is at 37.5° N, and the coverage of the area with a standard deviation > 4 is to the east of 90°E and between 30°−45° N, where the range of the EASWJ activities are concentrated. Therefore, the range of 90°−150° E, 30°−45° N is defined as the key area of the EASWJ. This is also consistent with previous research conclusions (Yang and Zhang [50]; Jin [19, 37]).

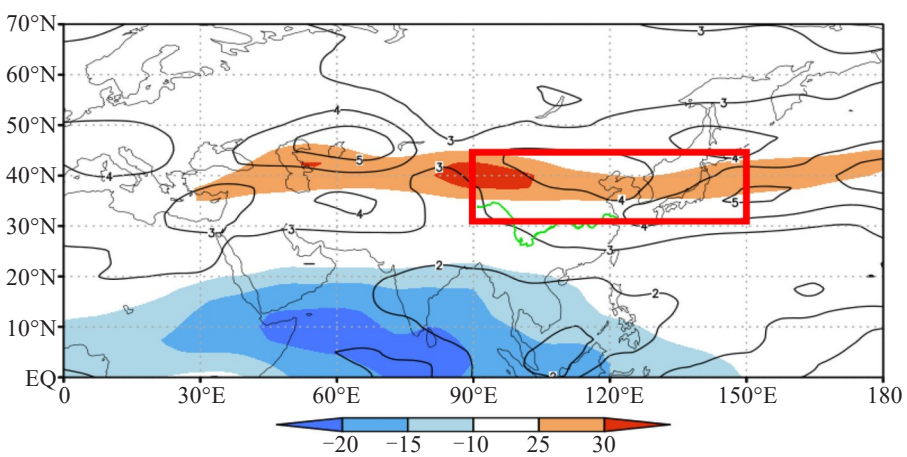

Figure 1. The 200 hPa zonal wind in June-July (JA) of 1960−2015 (shadow; red: > 30 m s^{-1}; blue: < −10 m s^{-1}) and its standard deviation (contour; unit: m s^{-1}). The red box represents the key area of the EASWJ.

Morlet wavelet analysis and the red noise test are carried out on the average daily data of the 200 hPa zonal wind in the EASWJ key areas during the Meiyu season (June-July) for the multi-year average, the seven wet Meiyu years and the four dry Meiyu years. It is found that the main periodic signals are 31−33 d, 30−32 d and 31−34 d, respectively. Low-frequency oscillations on a monthly scale (30−60 d) at middle and high latitudes are inherent characteristics of the atmosphere and play an important role in the evolution of weather and climate (Krishnamurti [51]; Li [17]). However, the significance of 30−60 d low-frequency oscillations suppresses the medium-term scale quasi-biweekly low-frequency and synoptic-scale variation signals, which are the focus time scales of this research. Therefore, the zonal wind is analyzed again by wavelet analysis after the signals above the 30d scale are filtered. Fig. 2 shows the wavelet analysis of the 200 hPa zonal wind of the multi-year average, and wet and dry Meiyu years after the variation signals longer than 30 d are filtered out. Seen from the figure, much shorter time-scale periodic signals appear and the main periodic signals are of synoptic scale, 3−7 d for the multi-year average, 3−4 d and 8 d for the wet Meiyu years and 5−7 d for the dry Meiyu years. The sub-periodic signals are quasi-biweekly low-frequency signals, with scales of 10−13 d, 12−17 d and 10−11 d for the multi-year average, wet Meiyu years and dry Meiyu years, respectively. In addition, wavelet analysis is performed yearly for the 11 abnormal Meiyu years after the zonal wind with signals longer than 30 d is filtered out, and then significant periodic signals are accumulated for wet and dry Meiyu years, respectively. The synoptic-scale signals for the seven wet Meiyu years focus mainly on 4 d, 7 d and 8 d, while the synoptic-scale signals for the four dry Meiyu years are mainly on 4 d and 6 d. Another relatively concentrated periodic signal is the 10−15 d quasi-biweekly low-frequency signal. In short, during the medium-term scale atmospheric dynamic process, the evolution of the EASWJ in the Meiyu season is mainly characterized by 3−8 d synoptic scale and 10−15 d low-frequency variabilities. The following section is to analyze the wave packet distribution and energy propagation of Rossby waves based on these two time scales.

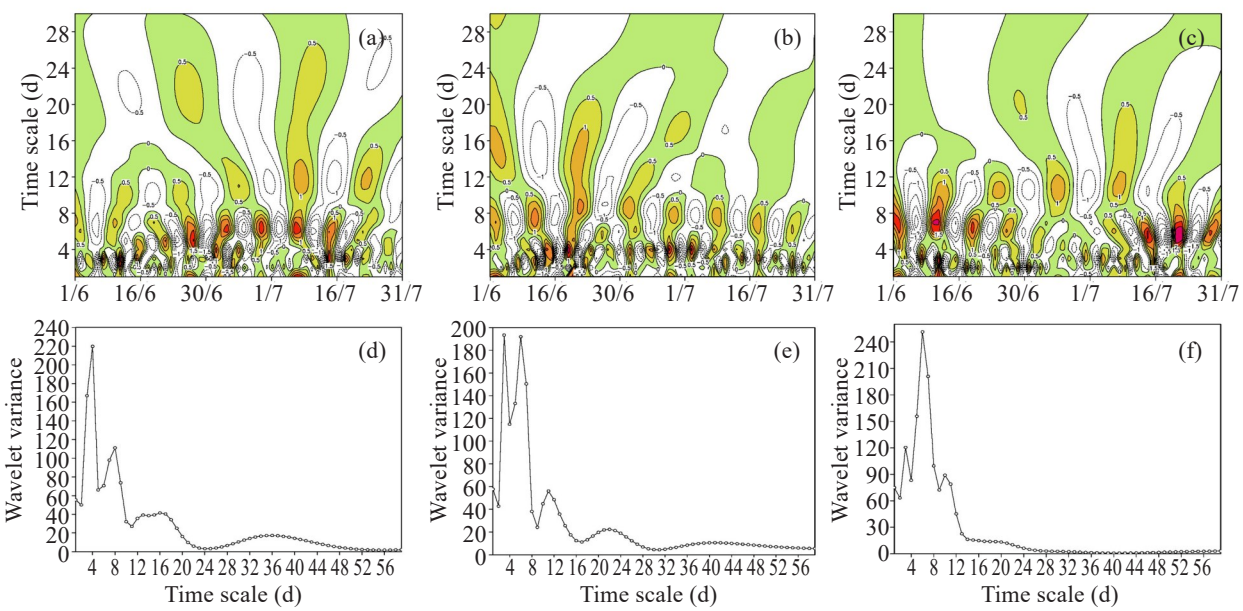

Figure 2. Wavelet analysis and variance sequence of the 200 hPa zonal wind in the key area of the EASWJ after filtering out variability above 30 d (a and d: multi-year average; b and e: wet Meiyu years; c and f: dry Meiyu years).

4 DISTRIBUTION OF PERTURBATION WAVE PACKETS OF ROSSBY WAVES ALONG THE EAST ASIAN SUBTROPICAL JET

4.1 *Distribution of the 3-8 d synoptic-scale perturbation wave packets*

Figure 3 presents the distribution of the 3−8 d synoptic-scale perturbation wave packets from the synthetic analysis of the 200 hPa zonal wind in June-July for the multi-year average, the seven wet and four dry Meiyu years. For the multi-year average (Fig. 3a), there is a large-value band for the perturbation wave packets in the middle and high latitudes (i.e., 35°−60°N) from Europe to North Pacific. The intensity of the perturbation wave packets along the ASWJ presents a high-low-high-low-high distribution pattern. The strongest area of the perturbation wave packets appears from the eastern part of Heilongjiang Province, China, to the western coast of the Okhotsk Sea. The area of the second highest intensity is located on the west coast of Europe to the Black Sea. There is a weak high-value center near the Lake Balkhash. The relatively low-value area appears within the three high-value regions, reflecting the wave train distribution of the 3−8 d

synoptic-scale perturbation energy on the ASWJ. In addition, it can be observed that the peak-value area of the perturbation wave packets is in East Asia (90°−150° E). The perturbation wave packets exhibit a high-low-high meridional wave train distribution from the tropical easterly belt to the subtropical westerly belt. The low-value band of the perturbation wave packets lies between two high-value bands of the perturbation wave packets on the tropical high-level easterly jet and the subtropical high-level westerly jet, corresponding to the eastern section of the South Asian high-pressure system in the upper troposphere, and reflecting the mode of low perturbation energy in the weak-wind region of the South Asian high-pressure system. Previously, a number of researchers have studied the two wave trains. Huang and Li [29], and Huang and Sun [31] pointed out that the quasi-stationary meridional wave train in East Asia, east of 90° E, was related to the East Asia-Pacific (EAP) teleconnection wave train. Enomoto et al. [32] referred to the zonal wave train structure on the Asian subtropical westerly jet as the "Silk Road" teleconnection. The zonal and meridional wave trains converge on the EASWJ, possibly indicating that Rossby wave activity on the EASWJ is an important dynamic mechanism for the weather and climate in East Asia.

The intensity of the synoptic-scale perturbation wave packets of the Rossby waves in wet Meiyu years (Fig. 3b) and dry Meiyu years (Fig. 3c) shows a high-low-high-low-high distribution pattern on the ASWJ as well. However, the phases of the wave trains along the ASWJ are different between wet Meiyu years and dry Meiyu years. The phase in wet Meiyu years is about 10°−15° longitude west of that in dry Meiyu years, and they are approximatively in opposite phases. For example, the areas near the Caspian Sea and Lake Balkhash are high-value areas of the wave packets in wet Meiyu years, but change into low-value areas of the wave packets in dry Meiyu years. In addition, the most intense area (value > 0.50) of the wave packets on the EASWJ is found between 40° − 50° N and 100° − 150° E in wet Meiyu years, but between 40°−75°N and 105°−160°E in dry Meiyu years when the wave packet intensity in the Okhotsk Sea area is even stronger. The high intensity of the wave packets means that there is an active long-wave trough (Song et al. [54]), which is not conducive to the formation of blocking high over the Okhotsk Sea and more rainfall during the Meiyu season (Tao and Wei [10]). In East Asia (90° − 150° E), the distribution of the wave packets in wet and dry Meiyu years also shows a high-low-high meridional wave-train structure, although the intensity of the tropical wave packet in dry Meiyu years is higher than that in wet Meiyu years. The intensity center contour in dry Meiyu years is 0.55 and that in wet Meiyu years is 0.45.

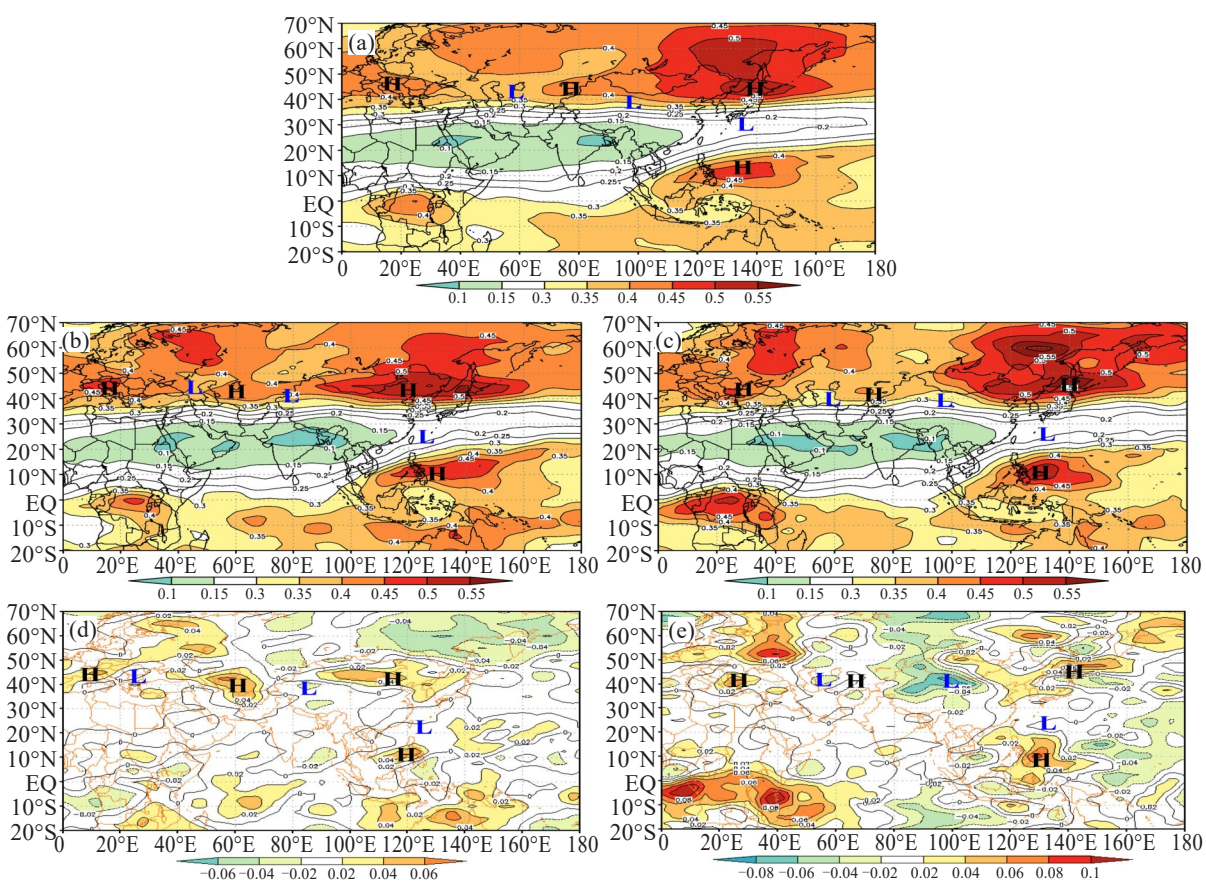

Figure 3. Synthetic analysis of the perturbation wave packets of 3−8 d synoptic-scale waves of the 200 hPa zonal wind in June-July for the multi-year average, wet Meiyu years, and dry Meiyu years (a: multi-year average, b: wet Meiyu years, c: dry Meiyu years, d and e: the same as b and c, respectively, but for the perturbation wave packet anomaly).

4.2 *Distribution characteristics of the 10–15 d low-frequency perturbation wave packets*

In the distribution diagram of the 10–15 d low-frequency perturbation wave packets (Fig.4), zonal high-low-high-low-high and meridional high-low-high wave trains are also found, and the differences between the patterns in wet Meiyu years and dry Meiyu years are more significant. In terms of zonal wave trains, the peak-value center of the wave packet intensity is located between the Aral Sea and the Lake Balkhash in wet Meiyu years. However, in dry Meiyu years the peak-value center is in northeast China, which indicates that the perturbation energy is concentrated upstream in wet Meiyu years, providing more energy and momentum for the development of downstream precipitation. Similarly, differences exist between the phases of the zonal wave trains, with the phase in wet Meiyu years being more systematically westward compared with that in dry Meiyu years. In terms of meridional wave trains, the wave packet values in wet Meiyu years are lower than those in dry Meiyu years.

It is seen that the 3–8 d synoptic scale, the 10–15 d low-frequency Rossby wave perturbation wave packets and the tropical perturbation wave packets in wet Meiyu years are all weaker than those in dry Meiyu years. The tropical perturbation wave packet is related to the easterly jet stream on the south side of the South Asian high-pressure area in the upper subtropical monsoon circulation and the easterly jet stream in the upper south branch of the tropical monsoon circulation (Fig. 1), both of which are part of the East Asian monsoon circulation system (Chen et al. [14]; He et al. [55]). The intensity of the perturbation wave packets is weak in wet Meiyu years, reflecting the weakening of the East Asian summer monsoon circulation. Zhang et al. [56-58] analyzed the relationship between the East Asian monsoon circulation system and the precipitation anomalies in the Yangtze-Huaihe River Basin during flood season, and concluded that when the East Asian summer monsoon circulation was weaker, precipitation in the Yangtze-Huaihe River Basin increased. The research by Huang and Li [52] also demonstrated that the EAP teleconnection was the result of the propagation of quasi-stationary planetary waves generated by the heat source forcing which was caused by severe convective activity around the Philippines in the Northern Hemisphere. In the case of severe convections over the tropical Western Pacific Ocean surrounding the Philippines in summer, precipitation in the Meiyu season in the Yangtze-Huaihe River Basin decreased, and vice versa. These theoretical analysis results are consistent with the facts revealed by the analysis of perturbation wave packets in this article.

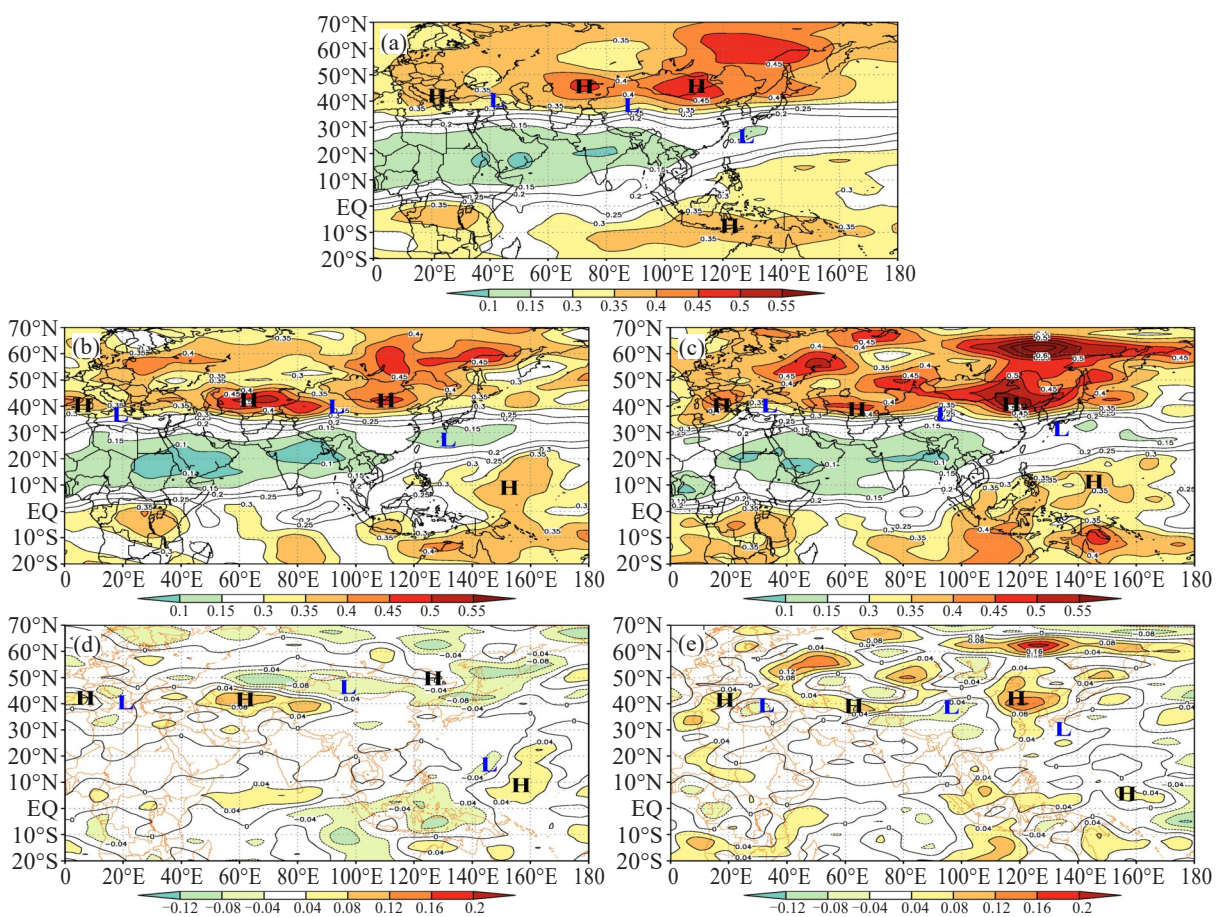

Figure 4. Synthetic analysis of the perturbation wave packets of 10–15 d low-frequency waves of the 200 hPa zonal wind in June-July for the multi-year average, wet Meiyu years and dry Meiyu years(a: multi-year average; b: wet Meiyu years; c: dry Meiyu years; d and e: the same as b and c, respectively, but for the perturbation wave packet anomaly).

5 ENERGY PROPAGATION OF ROSSBY WAVES ALONG THE EAST ASIAN SUBTROPICAL JET

Huang et al. [59] pointed out that the two most important teleconnections affecting the variation of summer climate in East Asia were the Silk Road teleconnection, which spread zonally along the Asian subtropical jet, and the EAP teleconnection that propagated meridionally across East Asia. Huang and Li [29, 52] first proved that the EAP teleconnection was caused by the propagation of the quasi-stationary planetary waves resulting from the heat source forcing which was generated by strong convection around the Philippines in the Northern Hemisphere. Subsequently, Enomoto et al. [53] put forward that the Silk Road teleconnection was the result of the quasi-stationary Rossby waves propagating along the ASWJ. Therefore, in the following section, we will investigate the energy propagation difference of the medium-term scale Rossby waves in wet Meiyu years and dry Meiyu years by using wave-activity flux, and also explore the formation mechanisms of the perturbation energy wave train.

Figure 5 shows the distributions of the 200 hPa horizontal wave-activity flux, its divergence, and the zonal wind during the Meiyu season (June-July) in wet and dry Meiyu years. The wave-activity flux along the ASWJ is basically eastward in the zonal direction, reflecting that the Rossby waves spread east along the jet and disperse downstream. The wave-activity flux divergences in wet Meiyu years and dry Meiyu years are distributed alternatively in convergence and divergence along the ASWJ. This phenomenon is corresponded with the zonal wave trains of the perturbation wave packets, proving the fact that the Silk Road teleconnection results from the quasi-stationary Rossby waves spreading along the ASWJ. In the East Asia region east of 90° E, the wave-activity flux is significantly enhanced, shown as strong wave-activity flux and its convergence and divergence. This reveals the significant enhancement of the energy propagation and wave-flow interaction in the East Asia region during the eastward propagation of the Rossby waves along the ASWJ. However, the wave-activity flux divergence distribution of 3−8 d synoptic-scale and 10−15 d low-frequency waves along the EASWJ in wet (dry) Meiyu years are in the pattern of "− + " ("+ − +"). Similarly, there is a "+ − +" meridional wave train distribution for the wave-activity flux divergence in both wet Meiyu years and dry Meiyu years in East Asia. Compared with the pattern in dry Meiyu years, the wave-activity flux and its divergence along the EASWJ in wet Meiyu years are stronger. Besides, the wave-activity flux along the EASWJ to the east of 120° E is divergent, and the jet intensity is stronger with core speed in excess of 30 m s^{-1} in wet Meiyu years, while the wave-activity flux divergence along the EASWJ to the east of 120° E is a convergent and a divergent zone in dry Meiyu years, and the strength of the jet stream is weak with core speed in excess of 25 m s^{-1} in dry Meiyu years. The wave-activity flux divergence and wave-flow interaction of the synoptic-scale variability in wet Meiyu years are stronger than those of the low-frequency variability, while the situation in dry Meiyu years tends to be the opposite. In addition, it is found that, in East Asia, the meridional propagation of the wave-activity flux is greater than its zonal propagation, and there are significant differences between the propagation paths of the wave activities in wet Meiyu years and dry Meiyu years. The wave-activity flux in wet Meiyu years moves from the area of the Ural Mountains to the southwest, entering the EASWJ near 100° E, and then continues to cross southeast through the jet, reaching the Yangtze-Huaihe River Basin in China and further southward to the sea near the Philippines. The synoptic-scale and low-frequency wave-activity fluxes over the southern border of the EASWJ in Yangtze-Huaihe River Basin are not only strong, but also in the transition from divergence to convergence. This indicates that the jet has been strengthened and can provide perturbation energy and dynamic forcing conditions for the generation of continuous precipitation in the Yangtze-Huaihe River Basin. The wave-activity flux in dry Meiyu years goes into the EASWJ from the northwestern part of India to the northeast, branching around 100° E. One branch propagates eastward to the Okhotsk Sea across the Sea of Japan, while the other moves southeast through southwest China to the seas of southeast China. Over the Yangtze-Huaihe River Basin, the synoptic-scale and low-frequency wave-activity fluxes are divergent and relatively weak, thus it is not conducive to the formation of continuous precipitation.

Figures 6 and 7 present the synthetic analysis of the precipitation anomalies, the 100 hPa South Asian high, the 200 hPa westerly jet, the 500 hPa geopotential height and anomaly field, the vertically integrated water vapor transport anomalies, the water vapor flux divergence anomalies and the vertical circulation anomalies along 110° − 120° E during June-July in wet Meiyu years and dry Meiyu years. As mentioned above, the zonal wave trains of the perturbation wave packets on the EASWJ at 200 hPa in wet (dry) Meiyu years are systematically westward (eastward), and the energy center of the low-frequency variability lies between the Aral Sea and the Lake Balkhash (in the northeastern part of China) and propagates eastward. In wet (dry) Meiyu years, the wave-activity fluxis concentrated (diverged) over eastern China with high (low) intensity, and the westerly jet is strong and southward (weak and northward). Zhang et al. [21] pointed out that the location anomaly of the EASWJ in June is mainly affected by the phase change of the east-moving Rossby wave trains in the mid and high latitudes of the Eurasian continent. In July, the location anomaly of the East Asian subtropical high-level westerly jet is dominated by the phase change of

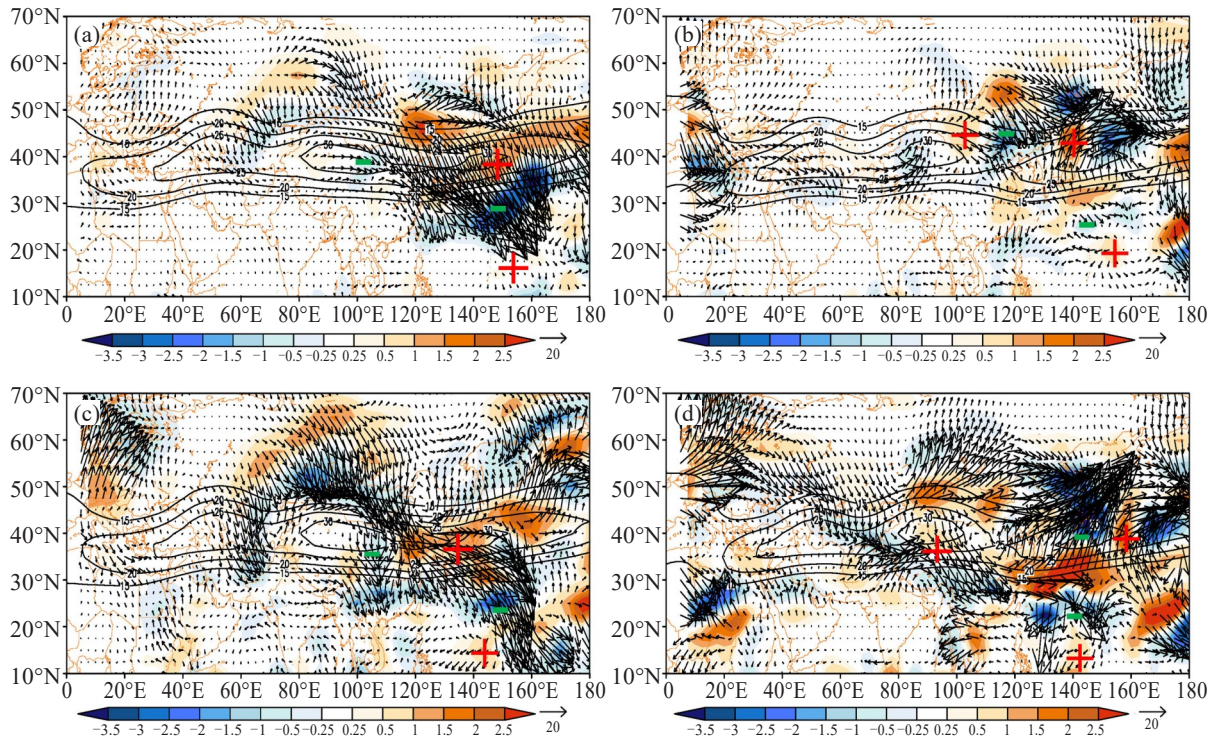

Figure 5. The 200 hPa horizontal wave-activity flux (vector; $m^2 s^{-2}$), wave-activity flux divergence (shadow; $10^{-6} m s^{-2}$; red plus (+) represents the divergence region; green minus (−) represents the convergence region) and average zonal wind (> 15 m s^{-1} contour), 3−8 d (a: wet Meiyu years; b: dry Meiyu years) and 10−15 d (c: wet Meiyu years; d: dry Meiyu years) during the Meiyu season (June-July).

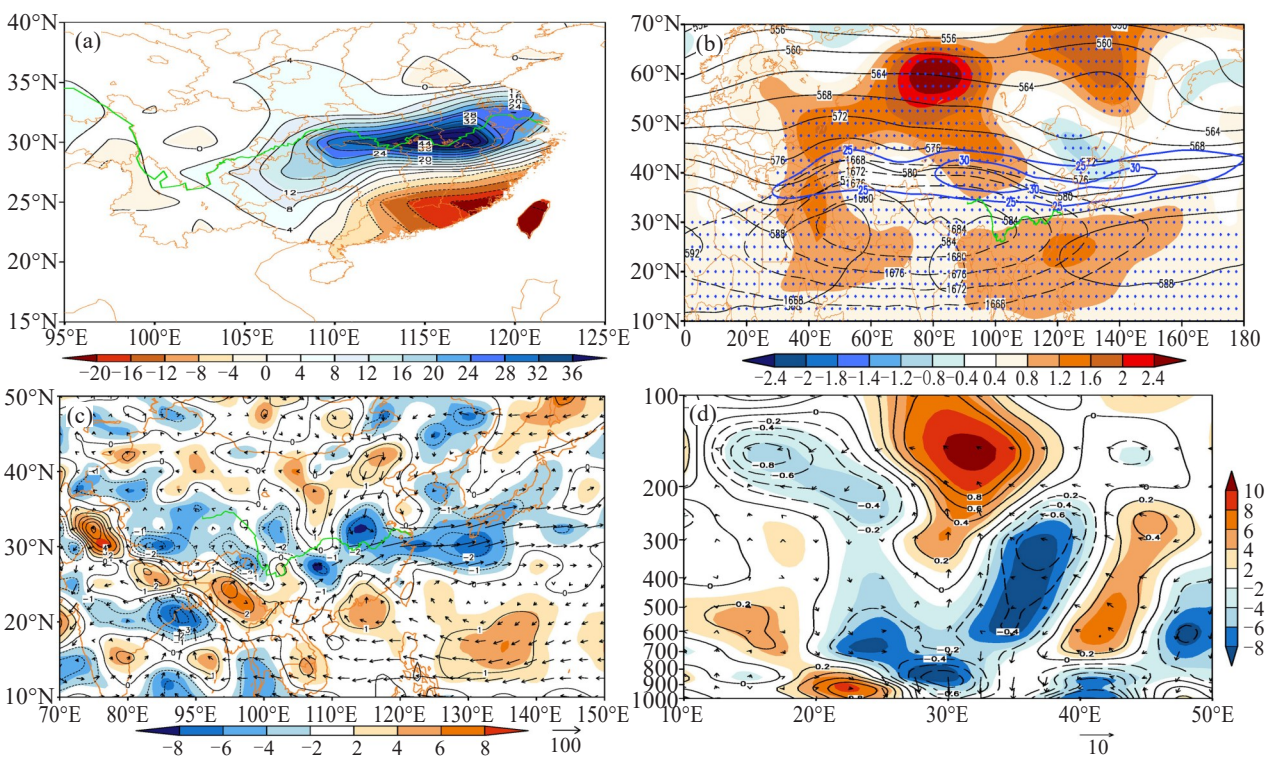

Figure 6. Synthetic analysis of (a) precipitation anomaly distribution; (b) 100 hPa geopotential height field (dashed line; unit: 10 gpm), 500 hPa geopotential height field (thin solid line; unit: 10 gpm), potential height anomaly field (shadow; unit: 10 gpm), and 200 hPa zonal wind field (thick solid line; unit: m s^{-1}). The black dots exceed the 95% confidence level; (c) vertically-integrated water vapor transport anomaly (arrow; unit: 10^{-4} kg m^{-1} s^{-1}) and water vapor flux divergence anomaly (contour; unit: 10^{-5} kg m^{-2} s^{-1}). Red(blue) shaded areas exceed the 95% confidence level; (d) vertical circulation (arrow) and divergence (contour, shadow; unit: 10^{-6} s^{-1}) from 110°−120°E in wet Meiyu years.

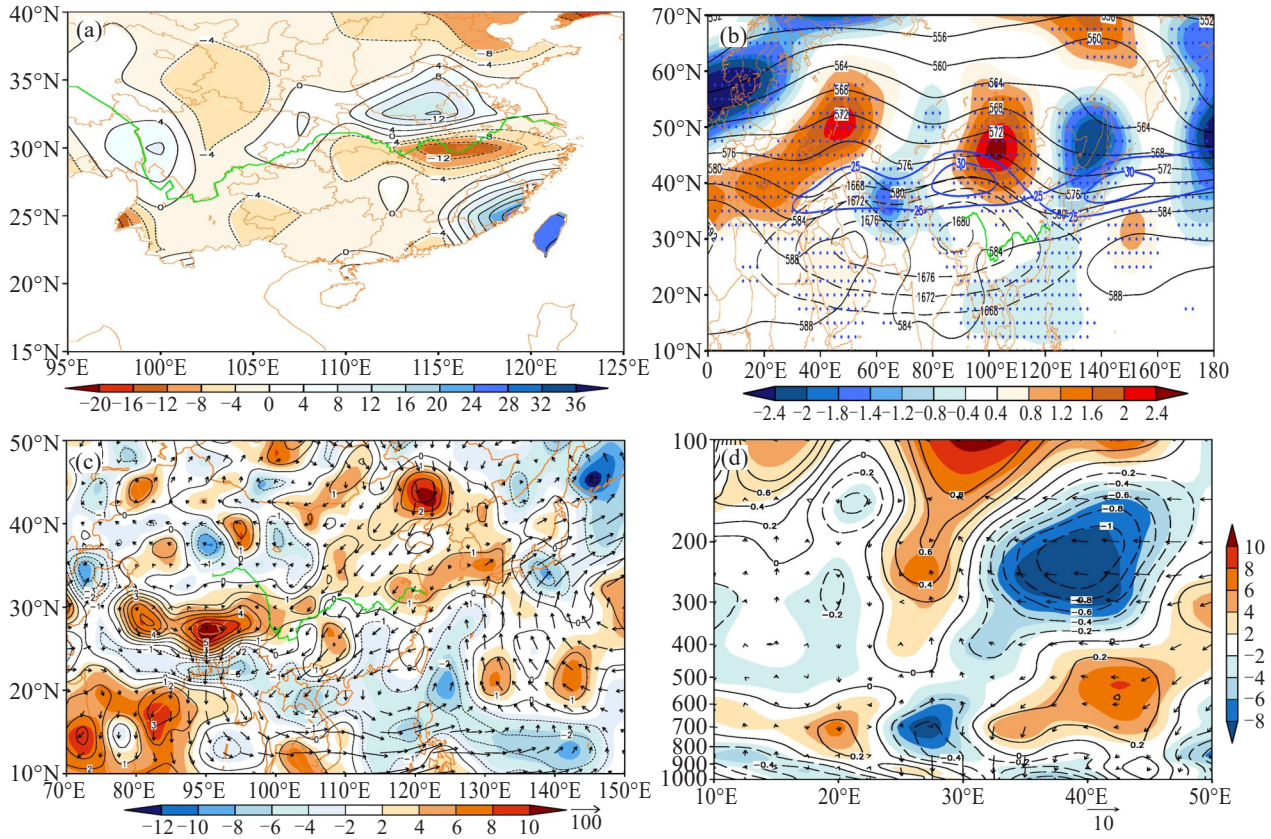

Figure 7. Synthetic analysis of (a) precipitation anomaly; (b) 100 hPa geopotential height field (dashed line; unit: 10 gpm), 200 hPa zonal wind field (thick solid line; unit: m s^{-1}), and 500 hPa geopotential height field (thin solid line; unit: 10 gpm), potential height anomaly field (shadow; unit: 10 gpm). The black dots exceed the 95% confidence level; (c) vertically-integrated water vapor transport anomaly (arrow; unit: 10^{-4} kg m^{-1} s^{-1}) and water vapor flux divergence anomaly (contour; unit: 10^{-5} kg m^{-2} s^{-1}). Red(blue) shaded areas exceed the 95% confidence level; (d) vertical circulation (arrow) and divergence (contour, shadow; unit: 10^{-6} s^{-1}) from 110°−120°E in dry Meiyu years.

the Rossby wave trains propagating from the tropical to subtropical regions of the western Pacific. Thus, it is deduced that the location anomaly of the EASWJ is influenced by the zonal and meridional Rossby wave trains during the Meiyu season. As the consequence of coupling of high and low level atmosphere and high-level strong (weak) divergence on the south side of the jet, low-level southwest wind is strengthened (weakened), leading to convergence (divergence) anomalies of the vertically-integrated water vapor flux in the Yangtze-Huaihe River Basin. In addition, there is strong divergence (zero dispersion) in the upper layers and strong (weak) convergence in the lower layers, which enhances (weakens) vertical ascending motion, providing favorable (unfavorable) dynamical conditions for rainfall during the Meiyu season in the Yangtze-Huaihe River Basin (Jin et al. [19]). At the same time, for the wet (dry) Meiyu years, the southern portion of the EASWJ at 200 hPa has a wave-activity flux convergence (divergence), which is favorable for strong (weak) and eastward (westward) shift of the South Asian high, and thus the northwest Pacific subtropical high is strengthened (weakened) and shifts westward (eastward), which is (is not) conducive to the steady maintenance of the circulation during the Meiyu season in the Yangtze-Huaihe River Basin, inducing more (less) Meiyu rainfall (Yang and Zhang [50, 60]).

Table 1. Impacts of perturbation wave train and energy propagation along the EASWJ on wet and dry Meiyu anomalies.

	Wet Meiyu years	Dry Meiyu years
Perturbation wave train on the EASWJ	By west	By east
Wave-activity flux divergence distribution along the EASWJ	“− +”	“+ − +”
Westerly jet at 200 hPa	Strong and southward	Weak and northward
Low-level southwest wind	Strengthened	Weakened
Vertically-integrated water vapor flux anomalies	Convergence	Divergence
Vertical ascending motion	Enhanced	Weakened

6 CONCLUSIONS

This paper has comparatively analyzed the wave packet distribution and energy propagation characteristics of the medium-range scale Rossby waves along the EASWJ in wet Meiyu years and dry Meiyu years by using the NCEP/NCAR daily reanalysis dataset and the daily precipitation in China. Their influences on the key circulation system and vertical structure of abnormal Meiyu have also been investigated. The main conclusions are as follows:

(1) During the medium-term scale atmospheric dynamic process in the Meiyu season, the evolution of the EASWJ is mainly featured with the variation of 3−8 d synoptic-scale and 10−15 d low-frequency Rossby waves after the 200 hPa zonal wind variations longer than 30 d are filtered out. For the 3−8 d synoptic-scale and 10−15 d low-frequency Rossby waves, the perturbation wave packet intensity along the ASWJ exhibits a high-low-high-low-high zonal wave train distribution and a high-low-high meridional wave train over East Asia (90° − 150° E), where the zonal and meridional wave trains converge on the EASWJ. The zonal wave train in wet Meiyu years is about 10°−15° to the west in dry Meiyu years, being close to the inverse phase. The energy center of low-frequency variability in wet (dry) Meiyu years is between the Aral Sea and the Lake Balkhash (in the northeast region of China), and the energy is concentrated in the upstream (downstream) to Meiyu rainfall area, China.

(2) The wave-activity flux is eastward along the ASWJ, with its divergence and convergence distributed alternatively, corresponding to the zonal wave train distribution of perturbation wave, reflecting that Rossby wave energy propagation along the ASWJ is an important dynamic mechanism for zonal wave train formation. The Rossby waves have the most significant energy propagation and wave-flow interaction in East Asia during their spreading eastward along the ASWJ, featuring strong wave-activity flux and its associated divergence. However, compared with the situation in dry Meiyu years, both the wave-activity flux and its divergence along the EASWJ in wet Meiyu years are much stronger, and the westerly jet is more powerful and southward. Due to the coupling of high and low level atmosphere and high-level strong (weak) divergence on the south side of the jet over the Yangtze-Huaihe River Basin, low-level southwest wind and the vertical ascending motion are strengthened (weakened), favorable (unfavorable) for precipitation increase during the Meiyu season in the Yangtze-Huaihe River Basin.

Finally, it should be noted that there are not enough samples of dry Meiyu years (only four samples), which may affect the representativeness of the findings of this research. Therefore, further work is needed to verify the results of this research in the future.

Acknowledgments: We thank Professor XIAO Tian-gui from Chengdu University of Information Technology for his guidance. Besides, we thank the reviewers for their constructive comments that lead to improvements to this paper.

REFERENCES

[1] BERGGREN R, GIBBS W J, NEWTON C W. Observational Characteristics of the Jet Stream [Z]. WMO Technical Note, 1958.

[2] ENDLICH R M, MCLEAN G S. The structure of the jet stream core [J]. J Atmos Sci, 1957, 14(6): 543-552, https://doi.org/10.1175/1520-0469(1957)0142.0.CO;2.

[3] HUANG S S, YU Z H. On the structure of the sub-tropical highs and some associated aspects of the general circulation of atmosphere [J]. Acta Meteor Sinica, 1962, 31 (4): 67-87 (in Chinese).

[4] GAO S T, TAO S Y, DING Y H. Generalized E-P flux characterizing wave-flow interaction [J]. Sci China (Series B), 1989, 19(7): 774-784 (in Chinese).

[5] GAO S T, TAO S Y, DING Y H. Upper wave-East Asian jet interaction during the period of cold wave outbreak [J]. Chin J Atmos Sci, 1992, 16(6): 718-724 (in Chinese), https://doi.org/10.3878/j.issn.1006-9895.1992.06.09.

[6] PATRICK K. Novel Perspectives of Jet-Stream Climatologic and Events of Heavy Precipitation on the Alpine Southside [D]. Zurich: Swiss Federal Institute of Technology (ETH), 2004.

[7] DING Y H, ZHAO S M, HE S X. Study on the multi-year average circulation of global tropical and subtropical 200 hPa from May to October (I) - Planet-scale circulation system [J]. Chin J Atmos Sci, 1988, 12(2): 174-181 (in Chinese), https://doi. org / 10.3878 / j. issn. 1006-9895.1988.02.09.

[8] TAN J L, JIANG J, YUAN J P. The seasonal, interannual and interdecadal variations of the intensity of different subtropical upper jet-stream centers [J]. Scientia Meteor Sinica, 2009, 29(4): 482-489 (in Chinese), https://doi.org/10.1016/S1003-6326(09)60084-4.

[9] LAU K M, BOYLE J S. Tropical and extratropical forcing of the large-scale circulation: A diagnostic study [J]. Mon Wea Rev, 1987, 115(2): 400-428, https://doi.org/10.1175/1520-0493(1987)115<0400:taefot>2.0.co;2.

[10] TAO S Y, WEI J. The westward northward advance of the subtropical high over the West Pacific in summer [J]. J Appl Meteor Sci, 2006, 17(5): 513-525 (in Chinese), https://doi.org/10.3969/j.issn.1001-7313.2006.05.001.

[11] YE D Z, TAO S Y, LI M C. The abrupt change of circulation over northern hemisphere during June and October [J]. Acta Meteor Sinica, 1958, 29(4): 27-41 (in Chinese).

[12] SHENG C Y. General Climate in China [M]. Beijing: Science Press, 1986 (in Chinese).

[13] CHEN L X. The structure of the East Asian monsoon circulation system and its medium-term changes [J]. Acta Oceanologica Sinica, 1984, 6(6): 744-758 (inChinese).

[14] CHEN L X, ZHU Q G, LUO H B. East Asian Monsoon [M]. Beijing: China Meteorological Press, 1991: 362 (in Chinese).

[15] TAO S Y, CHEN L X. The structure of general circulation over continent of Asia in summer [J]. Acta Meteor Sinica, 1957, 28: 233-247 (in Chinese), https://doi.org/10.11676/

qxxb1957.019.

[16] TAO S Y, ZHAO S X, ZHOU X P, et al. The research progress of the synoptic meteorology and synoptic forecast [J]. Chin J Atmos Sci, 2003, 27(4): 451-467 (in Chinese), https://doi. org / 10.3878 / j. issn. 1006-9895.2003.04.03.

[17] LI C Y, WANG Z T, LIN S Z, et al. The relationship between East Asian summer monsoon activity and northward jump of the upper westerly jet location [J]. Chin J Atmos Sci, 2004, 28(5): 641-658 (in Chinese), https://doi.org/10.3878/j.issn.1006-9895.2004.05.01.

[18] KUANG X Y, ZHANG Y C. Impact of the position abnormalities of East Asian subtropical westerly jet on summer precipitation in middle-lower reaches of Yangtze River [J]. Plateau Meteor, 2006, 25(3): 382-389 (in Chinese), https://doi. org / 10.3321 / j. issn: 1000-0534.2006.03.004.

[19] JIN R H, LI W J, ZHANG B, et al. A study of the relationship between East Asia subtropical westerly jet and abnormal Meiyu in the middle-lower reaches of the Yangtze River [J]. Chin J Atmos Sci, 2012, 36(4): 722-732 (in Chinese), https://doi. org / 10.3878 / j. issn. 1006-9895.2011.11076.

[20] GUO H, ZHANG Q Y. The dominant modes of precipitation anomalies in Eastern China during the peak of pre-rainy season in South China and possible causes [J]. Climatic Environ Res, 2016, 21(6): 633-652 (in Chinese), https://doi. org / 10.3878 / j. issn. 1006-9585.2016.16032.

[21] ZHANG Q Y, XUAN S L, SUN S Q. Anomalous circulation characteristics of intraseasonal variation of East Asian subtropical westerly jet in summer and precursory signals [J]. Chin J Atmos Sci, 2018, 42(4): 935-950 (in Chinese), https://doi.org/10.3878/j.issn.1006-9895.1803.18107.

[22] HOSKINS B J, KAROLY D J. The steady linear response of a spherical atmosphere to thermal and orographic forcing [J]. J Atmos Sci, 1981, 38(6): 1179-1196, https://doi. org / 10.1175 / 1520-0469(1981)038<1179: TSLROA>2.0.co;2.

[23] HOSKINS B J, AMBRIZZI T. Rossby wave propagation on a realistic longitudinally varying flow [J]. J Atmos Sci, 1993, 50(12): 1661-1671, https://doi. org / 10.1175 / 1520-0469(1993)050<1661:rwpoar>2.0.co;2.

[24] AMBRIZZI T, HOSKINS B J, HSU H H. Rossby wave propagation and teleconnection patterns in the austral winter [J]. J Atmos Sci, 1995, 52(21): 3661-3672, https://doi. org / 10.1175 / 1520-0469(1995)052<3661: RWPATP>2.0.CO;2.

[25] CHANG E K M. Characteristics of wave packets in the upper troposphere, Part II: Seasonal and hemispheric variations [J]. J Atmos Sci, 1999, 56(11): 1729-1747, https://doi.org/10.1175/1520-0469(1999)056<1729:cowpit>2.0.co;2.

[26] TERAO T. The zonal wavelength of the quasi-stationary Rossby wave trapped in the westerly jet [J]. J Meteor Soc Japan, 1999, 77: 687-699, https://doi. org / 10.2151 / jmsj1965.77.3_687.

[27] LU R Y, OH J H, KIM B J: A teleconnection pattern in upper-level meridional wind over the North African and Eurasian continent in summer [J]. Tellus, 2002, 54A: 44-55, https://doi.org/10.3402/tellusa.v54i1.12122.

[28] NITTA T. Convective activities in the tropical western Pacific and their impact on the northern hemisphere summer circulation [J]. J Meteor Soc Japan, 1987, 65(3): 373-390.

[29] HUANG R H, LI W J. Influence of the heat source anomaly over the tropical western Pacific on the subtropical high over East Asia [C]// International Conference on the General Circulation of East Asia. Chengdu: Institute of Atmospheric Physics, Chinese Academy of Sciences, 1987: 40-51.

[30] HUANG R H, SUN F Y. Interannual variation of the summer teleconnection pattern over the Northern Hemisphere and its numerical simulation [J]. Chin J Atmos Sci, 1992, 16(1): 52-61 (in Chinese), https://doi.org/10.3878/j.issn.1006-9895.1992.01.08.

[31] HUANG R H, SUN F Y. Impacts of the thermal state and the convective activities in the tropical western warm pool on the summer climate anomalies in East Asia [J]. Chin J Atmos Sci, 1994, 18(2): 141-151 (in Chinese), https://doi.org/10.1007/BF02658170.

[32] TAO S Y, WEI J, LIANG F, et al. Analysis of high impact weather induced by the downstream effect of Rossby waves [J]. Meteor Mon, 2010, 36(7): 81-93 (in Chinese), https://doi.org/10.7519/j.issn.1000-0526.2010.7.015.

[33] MEI S L, GUAN Z Y. Propagation of baroclinic wav packets in upper troposphere during the Meiyu period of 1998 over middle and lower reaches of Yangtze river valley [J]. J Trop Meteor, 2009, 25(3): 300-306(in Chinese), https://doi. org / 10.3969 / j. issn. 1004-4965.2009.03.007.

[34] XU J P, WANG W, CAI X J, et al. A Comparison of the Rossby wave activities and circulation features of the drought in winter-spring of 2011 and in summer of 2013 over mid-lower reaches of the Yangtze river basin [J]. J Trop Meteor, 2017, 33(6): 992-999 (in Chinese), https://doi.org/10.16032/j.issn.1004-4965.2017.06.020.

[35] KALNAY E, KANAMITSU M, KISTLER R, et al. The NCEP / NCAR 40-year reanalysis project [J]. Bull Amer Meteor Soc, 1996, 77(3): 437-471, https://doi. org / 10.1175/1520-0477(1996)077<0437:TNYRP>2.0.CO;2.

[36] XU Q, YANG Y W, YANG Q M. The Meiyu in middle-lower reaches of Yangtze River during 116 recent years (I) [M]// LIU Z C(ed), Torrential Rain · Disaster. Beijing: China Meteorological Press, 2001: 44-53 (in Chinese).

[37] JIN R H. Middle-Range Variation of The East Asian Subtropical Westerly Jet and Its Influence on Abnormal Character of Meiyu [M]. Nanjing: Nanjing University of Information Science and Technology, 2012.

[38] DING Y H, LIU J J, SUN Y, et al. A study of the synoptic-climatology of the Meiyu system in East Asia [J]. Chin J Atmos Sci, 2007, 31(6): 1082-1101(in Chinese), https://doi. org / 10.3878 / j. issn. 1006-9895.2007.06.05.

[39] LI Y, JIN R H, ZHOU N F, et al. An analysis on characteristics of heavy rainfall processes during the Meiyu season in Jianghuai region [J]. Acta Meteor Sinica, 2017, 75(5): 717-728 (in Chinese), https://doi. org / 10.11676/qxxb2017.052.

[40] TORRENCE C, COMPO G P. A practical guide to wavelet analysis [J]. Bull Amer Meteor Soc, 1998, 79: 61-78, https://doi.org/10.1175/1520-0477(1998)07960;0061:apgtwa62;2.0.co;2.

[41] GE F, XIAO T G, JIN R H, et al. Propagation and accumulation of perturbation energy in the severe cold surge, ice snow and frozen disaster in South China during January 2008 [J]. Meteor Mon, 2008, 34(12): 11-20(in Chinese), https://doi. org / 10.7519 / j. issn. 1000-0526.2008.12.002.

[42] XIAO T G, SUN Z B, GE F. The characteristic of wave packet propagation in 2008 Sichuan "Sep. 22" heavy rainfall process [J]. Scientia Meteor Sinica, 2010, 30(2): 185-192 (in Chinese), https://doi.org/10.3969/j.issn.1009-0827.2010.02.007.

[43] MIAO J H, XIAO T G, LIU Z Y. Theoretic foundation and computational method about the wave-packet propagation diagnosis [J]. Acta Meteor Sinica, 2002, 60 (4): 461-467 (in Chinese), https://doi. org / 10.11676 / qxxb2002.054.

[44] PLUMB R A. On the three-dimensional propagation of stationary waves [J]. J Atmos Sci, 1985, 42(3): 217-229, https://doi. org / 10.1175 / 1520-0469(1985)042<0217: OTTDPO>2.0.CO;2.

[45] TAKAYA K, NAKAMURA H. A formulation of a wave-activity flux for stationary Rossby waves on a zonally varying basic flow [J]. Geophys Res Lett, 1997, 24(23): 2985-2988, https://doi.org/10.1029/97gl03094.

[46] ELIASSEN A, PALM E. On the transfer of energy in stationary mountain waves [J]. Geofys Publ, 1961, 22(1): 1-23.

[47] HUANG R H. The conservation equation of wave action of planetary waves in spherical atmosphere and the stationary planetary wave propagation waveguide characterized by wave action flux [J].Sci China (B), 1984, 14(8): 766-775 (in Chinese), https://doi. org / 10.1360 / zb1984-14-8-766.

[48] LI C Y. Intraseasonal oscillations in the atmosphere [J]. Chin J Atmos Sci, 1990, 14(1): 32-45 (in Chinese), https://doi.org/10.3969/j.issn.1006-9585.2000.04.005.

[49] LI C Y. Introduction to Climate Dynamics (Second Edition) [M]. Beijing: Science Press, 2000 (in Chinese).

[50] YANG L M, ZHANG Q Y. Relationships between perturbation kinetic energy anomaly along East Asian westerly jet and subtropical high in summer [J]. J Appl Meteor Sci, 2007, 18(4): 452-459 (in Chinese), https://doi. org/10.3969/j.issn.1001-7313.2007.04.005.

[51] KRISHNAMURTI T N. Summer monsoon experiment-a review [J]. Mon Wea Rev, 1985, 113(9): 1590-1626.

[52] HUANG R H, LI W J. Influence of heat source anomaly over the western tropical Pacific on the subtropical high over East Asia and its physical mechanism [J]. Chin J Atmos Sci, 1988, 12(s1): 107-116(in Chinese), https://doi. org/10.3878/j.issn.1006-9895.1988.t1.08.

[53] ENOMOTO T, HOSKINS B J, MATSUDA Y. The formation mechanism of the Bonin high in August [J]. Quart J Roy Meteor Soc, 2003, 129(587): 157-178, https: //doi.org/10.1256/qj.01.211.

[54] SONG Y, MIAO J H, JU J H. Relationships between features of wave packet propagation and movement of western Pacific subtropical high [J]. Acta Meteor Sinica, 2006, 64(5): 576-582 (in Chinese), https://doi. org / 10.11676/qxxb2006.056.

[55] HE J H, YU J J, SHEN X Y, et al. Research on mechanism and variability of east Asian monsoon [J]. J Trop Meteor, 2004, 20(5): 449-459 (in Chinese), https:// doi.org/10.3969/j.issn.1004-4965.2004.05.001.

[56] ZHANG Q Y, TAO S Y. Influence of Asian mid-high latitude circulation on East Asian summer rainfall [J]. Acta Meteor Sinica, 1998, 56(2): 199-211 (in Chinese), https://doi.org/10.1007/s00376-999-0032-1.

[57] ZHANG Q Y, TAO S Y. The study of the sudden northward jump of the subtropical high over the western Pacific [J]. Acta Meteor Sinica, 1999, 57(5): 539-548 (in Chinese), https://doi.org/10.1007/s00376-999-0032-1.

[58] ZHANG Q Y, TAO S Y, ZHANG S L. The persistent heavy rainfall over the Yangtze River valley and its associations with the circulations over East Asian during summer [J]. Chin J Atmos Sci, 2003, 27(6): 1018-1030 (in Chinese), https://doi. org / 10.3878 / j. issn. 1006-9895.2003.06.06.

[59] HUANG R H, HUANGFU J L, LIU Y, et al. Development from the theory of energy dispersion of Rossby waves to studies on the dynamics of quasi-stationary planetary waves [J]. Chin J Atmos Sci, 2016, 40 (1): 3-21 (in Chinese), https://doi.org/10.3878/j.issn.1006-9895.1503.14298.

[60] YANG L M, ZHANG Q Y. Climate features of summer Asia subtropical westerly jet stream [J]. Climatic Environ Res, 2008, 13(1): 10-20 (in Chinese), https://doi. org / 10.3878/j.issn.1006-9585.2008.01.02.

Citation: JIN Rong-hua, YANG Ning, SUN Xiao-qing, et al. The relationship between abnormal Meiyu and medium-term scale wave perturbation energy propagation along the East Asian subtropical westerly jet [J]. J Trop Meteor, 2020, 26(2): 125-136, https://doi.org/10.46267/j.1006-8775.2020.012.